

DIRECTED TRANSVERSE FLOW AND ITS DISAPPEARANCE FOR ASYMMETRIC REACTIONS

Lovejot^a, S. Gautam^{b, 1}

^a Department of Physics, Panjab University, Chandigarh, India

^b Dev Samaj College for Women, Sector 45 B, Chandigarh, India

We study the directed transverse flow for mass asymmetry reactions. This is done by keeping the target fixed and varying the projectile mass from ${}^4\text{He}$ to ${}^{131}\text{Xe}$. We find that directed transverse flow is sensitive to the mass of the projectile. We also study the disappearance of flow at a particular impact parameter called Geometry of Vanishing Flow (GVF) for such mass asymmetry reactions. Our results indicate that GVF is sensitive to the beam energy as well as to the mass of the projectile.

Изучается прямой поперечный поток для реакций с асимметричными массами. Это достигается путем фиксирования мишени и варьирования соударяемой массы от ${}^4\text{He}$ до ${}^{131}\text{Xe}$. Обнаружено, что прямой поперечный поток чувствителен к соударяемой массе. Также изучается исчезновение потока для определенных параметров соударения, называемых геометрией исчезающего потока, для таких реакций с асимметричными массами. Результаты показывают, что геометрия исчезающего потока чувствительна к энергии пучка так же, как и к соударяемой массе.

PACS: 24.50.+g

INTRODUCTION

It is now well accepted that collective transverse in-plane flow serves as one of the best candidates to study the properties of hot and dense nuclear matter. It is also known that collective flow is sensitive to equation of state and the measurements on flow have proved to be useful in constraining equation of state of symmetric nuclear matter [1]. In past three decades, extensive efforts have been carried out in both theoretical and experimental fronts regarding the behavior of collective flow with various entrance channel parameters such as incident energy [2, 3], colliding geometry [4, 5], system size [6, 7], mass [8] and isospin symmetry [9–11]. At low incident energies (i.e., few MeV/nucleon) dynamics is governed by the attractive mean field and flow is negative. At higher incident energies, flow is positive because of the dominance of repulsive nucleon–nucleon scattering. Therefore, while going from the low to higher incident energies, flow disappears at a particular incident energy. This is because of the counterbalancing of the attractive and repulsive interactions. This energy at

¹E-mail: sakshigautm@gmail.com

which disappearance of flow takes place is termed as the energy of vanishing flow (EVF) [12]. A large number of theoretical and experimental efforts have been carried out to study the energy of vanishing flow. Its dependence on the mass of colliding nuclei [13,14], colliding geometry [15], mass asymmetry of the reaction [8] and on isospin degree of freedom [10,16] has been studied extensively. Similar studies have been carried out regarding entrance channel dependence on elliptical flow [17] and multifragmentation [18].

Colliding geometry, on the other hand, also plays a significant role in directed flow and its disappearance. The directed flow first increases when we go from perfectly central to semi-central collisions, reaches a maximum at a particular value of the impact parameter, and again decreases as one moves to peripheral collisions. This is because of near absence of binary nucleon–nucleon collisions. The value of the impact parameter at which directed flow crosses zero is called geometry of vanishing flow (GVF) [19]. The GVF has been found to be dependent on the mass of the colliding nuclei. The mass dependence of GVF is found to be sensitive towards binary nucleon–nucleon cross section, thus pointing that GVF can be used as a probe to study in-medium nucleon–nucleon cross section [19]. On the other hand, the mass dependence of GVF has been found to be insensitive towards the nuclear matter equation of state. All the above-mentioned studies were restricted to symmetric reactions (same projectile and target nuclei).

Reaction dynamics also depends on the asymmetry between the projectile and target nuclei [8]. The excitation energy will be stored in the form of compressional energy in case of symmetric reactions, while most of the excitation energy will be in the form of thermal excitation energy for reactions involving asymmetric colliding nuclei. So we aim to study the behavior of GVF by simulating the asymmetric reactions, i.e, for different projectile and target nuclei. This is done by keeping the target fixed and varying the projectile from lighter to heavier masses. So the focus of the present work is

(i) to see how GVF behaves for the asymmetric reactions;

(ii) to see whether GVF still scales with the total mass of the colliding pair or with the mass of the projectile nuclei only (as the target nuclei is kept fixed). On the experimental front, such reaction studies can also be confirmed at Super Conducting Cyclotron at VECC, Kolkata, where we have the possibility of lighter beams. This study is carried out within the framework of quantum molecular dynamics (QMD) model which is discussed in the following section.

1. QUANTUM MOLECULAR DYNAMICS (QMD) MODEL

In QMD model, each nucleon propagates under the influence of mutual two- and three-body interactions. The propagation is governed by the classical equations of motion:

$$\dot{\mathbf{r}}_i = \frac{\partial H}{\partial \mathbf{p}_i}, \quad \dot{\mathbf{p}}_i = -\frac{\partial H}{\partial \mathbf{r}_i}, \quad (1)$$

where H stands for the Hamiltonian which is given by

$$H = \sum_i^A \frac{\mathbf{p}_i^2}{2m_i} + \sum_i^A (V_i^{\text{Skyrme}} + V_i^{\text{Yuk}} + V_i^{\text{Coul}} + V_i^{\text{mdi}}). \quad (2)$$

Here V_i^{Skyrme} , V_i^{Yuk} , V_i^{Coul} , and V_i^{mdi} are, respectively, the Skyrme, Yukawa, Coulomb, and momentum-dependent potentials. The momentum-dependent interactions are obtained by parameterizing the momentum dependence of the real part of the optical potential. The final form of the potential reads as [20]

$$U^{\text{mdi}} \approx t_4 \ln^2 [t_5 (\mathbf{p}_1 - \mathbf{p}_2)^2 + 1] \delta(\mathbf{r}_1 - \mathbf{r}_2). \quad (3)$$

Here $t_4 = 1.57 \text{ MeV}$ and $t_5 = 5 \cdot 10^{-4} \text{ MeV}^{-2}$. A parameterized form of the local plus mdi potential is given by

$$U = \alpha \left(\frac{\rho}{\rho_0} \right) + \beta \left(\frac{\rho}{\rho_0} \right) + \delta \ln^2 \left[\epsilon \left(\frac{\rho}{\rho_0} \right)^{2/3} + 1 \right] \frac{\rho}{\rho_0}. \quad (4)$$

The parameters α , β and γ are -124 , 70.5 and 2 for hard equation of state and -356 , 303 and 1.17 for soft equation of state.

The phase space of the nucleons is stored at several time steps and this is clustered using minimum spanning tree method that binds the nucleons, if they are closer than 4 fm in coordinate space.

2. RESULTS AND DISCUSSION

We simulated the reactions of ${}^4\text{He} + {}^{197}\text{Au}$, ${}^{12}\text{C} + {}^{197}\text{Au}$, ${}^{58}\text{Ni} + {}^{197}\text{Au}$, ${}^{92}\text{Zr} + {}^{197}\text{Au}$, and ${}^{131}\text{Xe} + {}^{197}\text{Au}$ at incident energies of 100 and 400 MeV/nucleon throughout the range of colliding geometry ($b/b_{\text{max}}(\hat{b}) = 0, 0.2, 0.4, 0.6$ and 0.8). For the present study, we used a soft equation of state along with energy-dependent Cugnon nucleon–nucleon cross section [21].

The transverse flow has been studied using couples of variables such as by investigating the slope of flow at mid-rapidity and also by investigating the product of rapidity and transverse momentum. It has been shown in [14] that both the methods are equivalent and yield same energy of vanishing flow. The transverse in-plane flow is calculated using *directed transverse momentum* $\langle p_x^{\text{dir}} \rangle$, which is defined as [14,22]

$$\langle p_x^{\text{dir}} \rangle = \frac{1}{A} \sum_{i=1}^A \text{sign} \{y(i)\} p_x(i), \quad (5)$$

where $y(i)$ and $p_x(i)$ are, respectively, the rapidity and the momentum of the i th particle. The rapidity is defined as

$$y(i) = \frac{1}{2} \ln \frac{\mathbf{E}(i) + \mathbf{p}_z(i)}{\mathbf{E}(i) - \mathbf{p}_z(i)}, \quad (6)$$

where $\mathbf{E}(i)$ and $\mathbf{p}_z(i)$ are, respectively, the energy and longitudinal momentum of the i th particle. In this definition, all the rapidity bins are taken into account.

In Fig. 1, we display the time evolution of $\langle p_x^{\text{dir}} \rangle$ for the collision of ${}^4\text{He} + {}^{197}\text{Au}$, ${}^{12}\text{C} + {}^{197}\text{Au}$, ${}^{58}\text{Ni} + {}^{197}\text{Au}$, ${}^{92}\text{Zr} + {}^{197}\text{Au}$, and ${}^{131}\text{Xe} + {}^{197}\text{Au}$ at different impact parameters of $b/b_{\text{max}} = 0.0$ (solid line), 0.2 (dashed line), 0.4 (dotted line), 0.6 (dash-dotted), 0.8 (dash-double-dotted) at a beam energy of 100 MeV/nucleon. From the figure, we see that $\langle p_x^{\text{dir}} \rangle$ remains zero at central collisions for all the reactions. The directed flow $\langle p_x^{\text{dir}} \rangle$ is negative initially which signifies the role of attractive mean field interactions during the initial phase

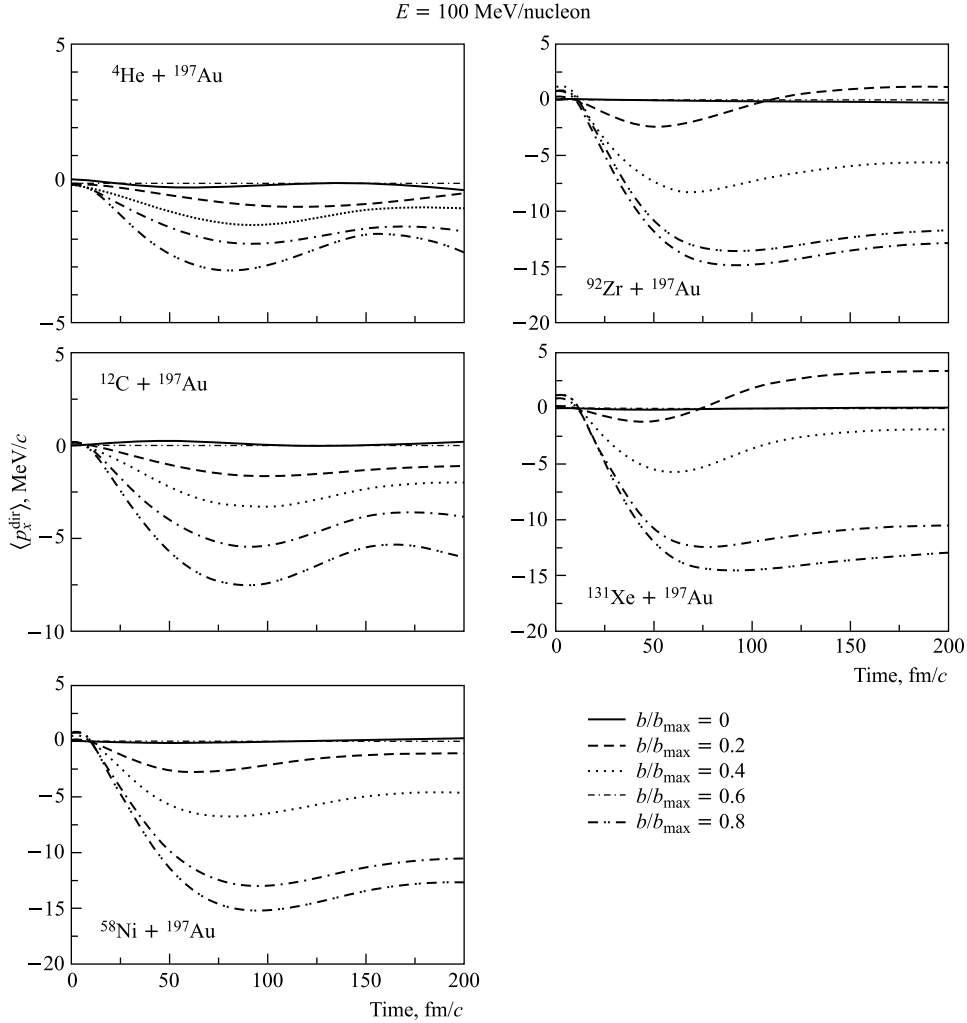


Fig. 1. The time evolution of the directed transverse flow $\langle p_x^{\text{dir}} \rangle$ for the reactions of ${}^4\text{He} + {}^{197}\text{Au}$, ${}^{12}\text{C} + {}^{197}\text{Au}$, ${}^{58}\text{Ni} + {}^{197}\text{Au}$, ${}^{92}\text{Zr} + {}^{197}\text{Au}$, and ${}^{131}\text{Xe} + {}^{197}\text{Au}$ at different impact parameters of $b/b_{\text{max}} = 0.0, 0.2, 0.4, 0.6, 0.8$ at a beam energy of 100 MeV/nucleon. Explanations are given in text

of the reaction. These interactions remain either attractive or may turn repulsive, depending on the incident energy. At energy of 100 MeV/nucleon, they remain negative throughout the time evolution for all the reacting pairs at all the colliding geometries. This is because of the less beam energy, which in turn, yields less binary nucleon–nucleon (nn) collisions.

In Fig. 2, we display the time evolution of $\langle p_x^{\text{dir}} \rangle$ for different colliding pairs as in Fig. 1, but at an incident energy of 400 MeV/nucleon. From the figure, we see that $\langle p_x^{\text{dir}} \rangle$ remains negative for the reactions of lighter projectiles on ${}^{197}\text{Au}$ target at almost all the colliding geometries. This implies that the interactions remain attractive throughout the reaction. On the other hand, for heavier projectiles like ${}^{58}\text{Ni}$, ${}^{92}\text{Zr}$ and ${}^{131}\text{Xe}$, the nn collisions will dominate the dynamics at final phase of the reaction at 400 MeV/nucleon and $\langle p_x^{\text{dir}} \rangle$ turns positive.

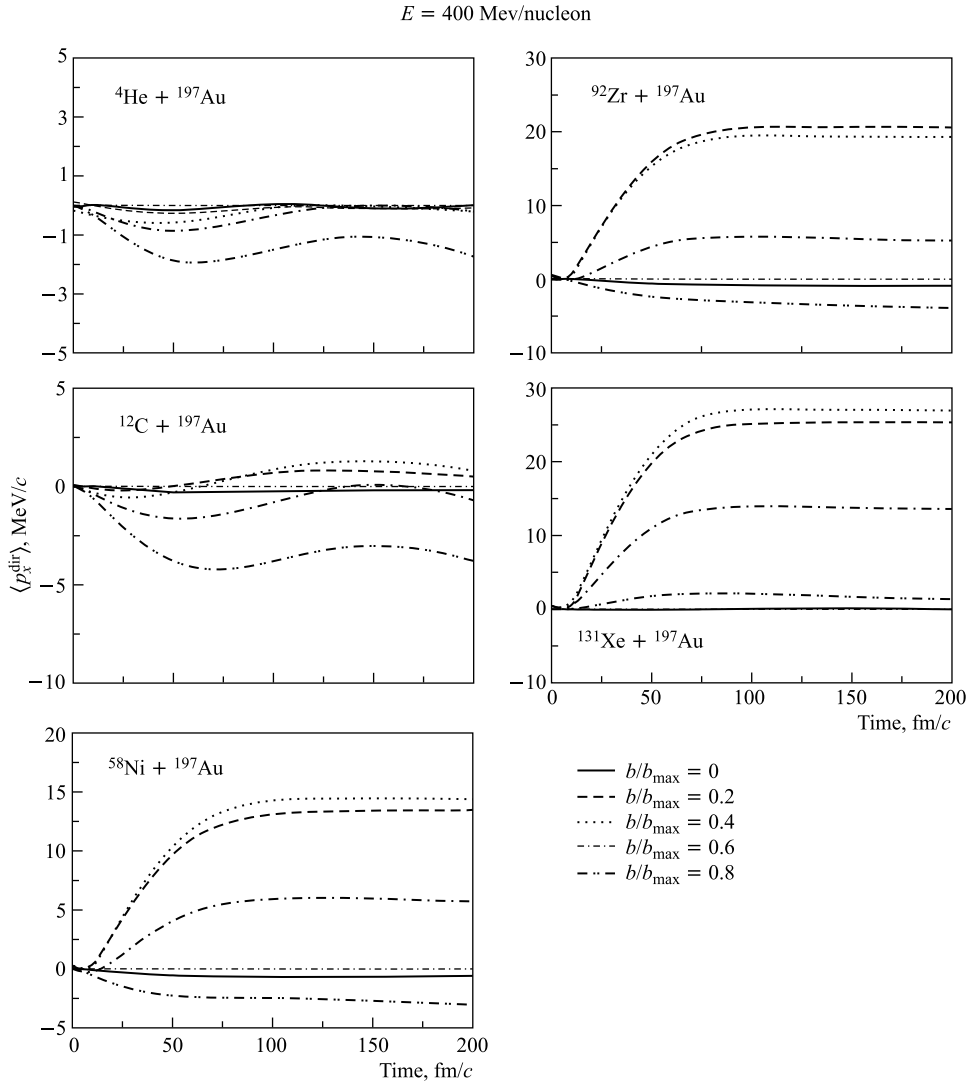


Fig. 2. Same as Fig. 2, but at a beam energy of 400 MeV/nucleon

In Fig. 3, we display the impact parameter dependence of $\langle p_x^{\text{dir}} \rangle$ for various reactions at 100 MeV/nucleon (panel *a*) and 400 MeV/nucleon (panel *b*). Squares, circles, triangles, pentagons and diamonds represent the collisions of ${}^4\text{He}$, ${}^{12}\text{C}$, ${}^{58}\text{Ni}$, ${}^{92}\text{Zr}$, and ${}^{131}\text{Xe}$, respectively, on ${}^{197}\text{Au}$ target. From the figure, we see that at 100 MeV/nucleon (Fig. 3, *a*) $\langle p_x^{\text{dir}} \rangle$ remains negative for the reactions of lighter projectiles like ${}^4\text{He}$, ${}^{12}\text{C}$ and ${}^{58}\text{Ni}$ on ${}^{197}\text{Au}$ throughout the range of colliding geometry and decreases when we go from central to peripheral collisions. This is because particles mainly emit from the body of much more heavier (than projectile) target. As we move to the reaction of heavier projectiles like ${}^{92}\text{Zr}$ and ${}^{131}\text{Xe}$ with ${}^{197}\text{Au}$ target, we see that $\langle p_x^{\text{dir}} \rangle$ increases when we move from perfectly central collisions to semi-central collisions, reaches a maximum and finally decreases and become negative

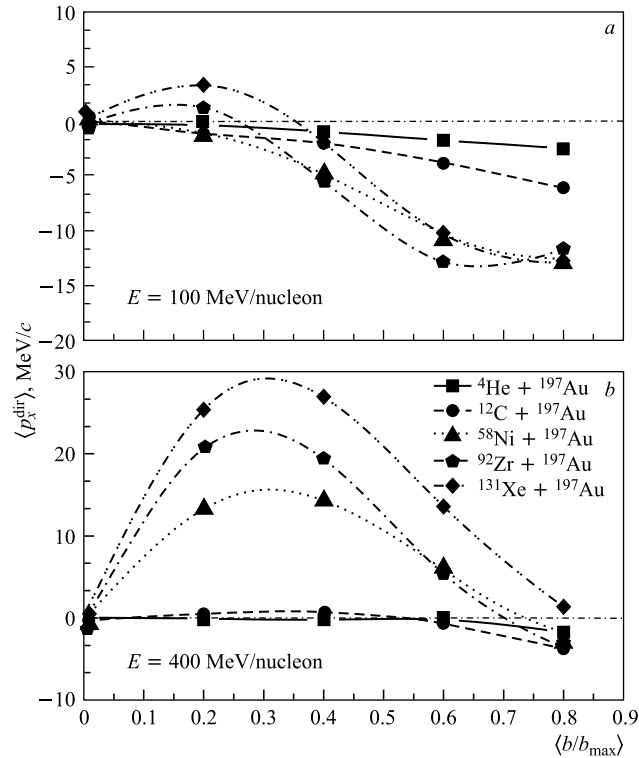


Fig. 3. Impact parameter dependence of transverse in-plane-flow $\langle p_x^{\text{dir}} \rangle$ at energies of 100 MeV/nucleon (a) and 400 MeV/nucleon (b) for various systems. Explanations are given in text

for peripheral collisions. This is because of the real absence of nucleon–nucleon collisions at peripheral geometry as explained earlier also. Also at 400 MeV/nucleon (Fig. 3, b), we see that the $\langle p_x^{\text{dir}} \rangle$ is more than that at 100 MeV/nucleon at all the colliding geometries for all the colliding pairs. This can be interpreted as the effect of increasing pressure gradient with increase in incident energy. From the figure, we also see that for all the reactions, $\langle p_x^{\text{dir}} \rangle$ first increases when we go from perfectly central collision to semi-central collision, reaches a maximum value at a particular value of impact parameter and then again decreases except for the reaction of very light projectile of ${}^4\text{He}$ on ${}^{197}\text{Au}$. For ${}^4\text{He} + {}^{197}\text{Au}$ collisions, $\langle p_x^{\text{dir}} \rangle$ is almost zero through the range of colliding geometry because the projectile nucleus is too light and so it cannot affect the heavy target ${}^{197}\text{Au}$ and flow remains zero. The value of impact parameter where $\langle p_x^{\text{dir}} \rangle$ crosses zero is called geometry of vanishing flow (GVF).

In Fig. 4, we display the GVF as a function of the total mass of the colliding nuclei ($A_P + A_T$) as well as with the mass of the projectile nucleus, where A_P and A_T are the mass of the projectile and target nuclei, respectively. From the figure, we see that the GVF increases with total mass of the colliding system ($A = A_P + A_T$) (panel a) as well as with the mass of the projectile nucleus (A_P) (panel b). This is because of the increasing pressure gradient for heavier projectiles. So it takes longer (more towards peripheral geometry) for the flow to vanish. Mass dependence of GVF follows a power law behavior ($\propto A^\tau$) where

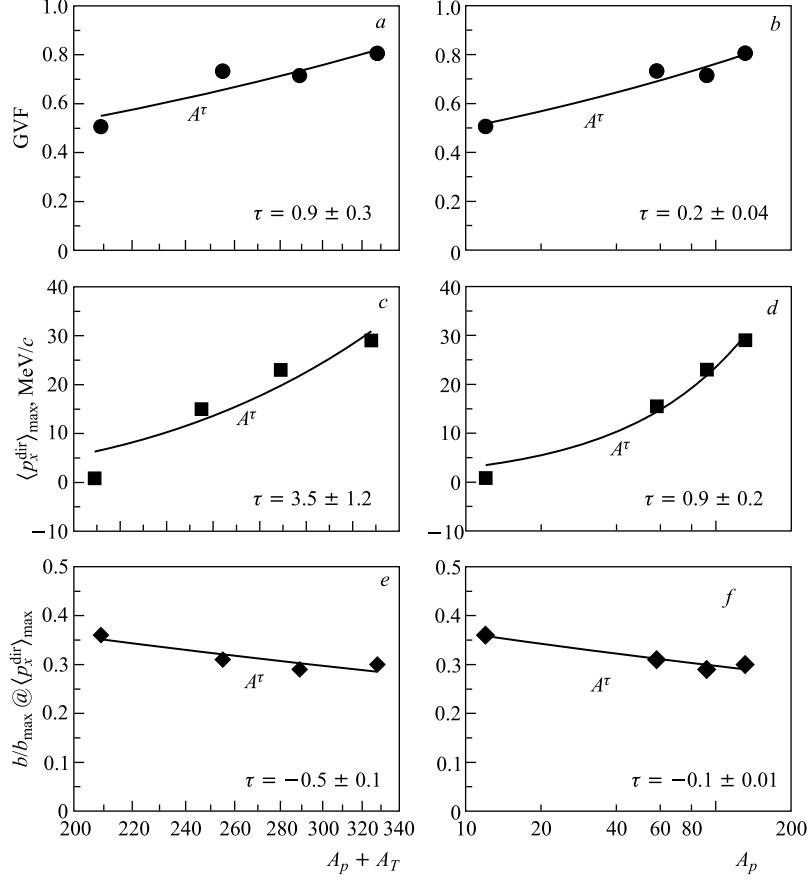


Fig. 4. System size dependence of the geometry of vanishing flow (GVF) (a, b), maximum value of $\langle p_x^{\text{dir}} \rangle$ (c, d) and \hat{b} at maxima of $\langle p_x^{\text{dir}} \rangle$ (e, f) at an incident energy of 400 MeV/nucleon

$\tau = 0.9 \pm 0.3$ for $A = A_P + A_T$ and $\tau = 0.2 \pm 0.04$ for $A = A_P$. In the middle panel, we show the maximum value of $\langle p_x^{\text{dir}} \rangle$ (labelled as $\langle p_x^{\text{dir}} \rangle_{\text{max}}$) as a function of total mass of the colliding nuclei ($A_P + A_T$) (panel c) and mass of the projectile (A_P) (panel d). The $\langle p_x^{\text{dir}} \rangle_{\text{max}}$ also increases with total mass as well as the projectile mass. The increase in $\langle p_x^{\text{dir}} \rangle_{\text{max}}$ is also because of increasing pressure gradient for heavier projectiles. The power law factor τ is 3.5 ± 1.2 and 0.9 ± 0.2 for $A = A_P + A_T$ and A_P , respectively. In the bottom panels, we display the system size dependence of the impact parameter at which $\langle p_x^{\text{dir}} \rangle$ becomes maximum (labelled as $b/b_{\text{max}} @ \langle p_x^{\text{dir}} \rangle_{\text{max}}$) as a function of the total mass ($A = A_P + A_T$) and the projectile mass ($A = A_P$). From the figure, we see that b/b_{max} decreases as the total system mass and the projectile mass increases and follows a power law behavior. When we go from central to peripheral collisions for heavier masses, the flow achieves maximum value earlier (towards central geometry). The power law factor $\tau = -0.5 \pm 0.1$ for $A = A_P + A_T$ and -0.1 ± 0.01 for $A = A_P$. From the above discussions, it is clear that GVF, maximum value of flow and the geometry at which the transverse momentum becomes maximum have shown a strong dependence on total system mass and relatively weak dependence on projectile nuclei.

3. SUMMARY

Using the quantum molecular dynamics model, we explored the dynamics of collective transverse flow in asymmetric reactions. We simulated the reactions by varying the projectile on fixed target Au. Our study reveals clear dependence of collective flow dynamics on the mass of the projectile and beam energy. Also, the geometry of vanishing flow and maximum value of transverse momentum is found to scale with mass of the projectile as well as total mass of the reacting system.

REFERENCES

1. *Danielewicz P., Lacey R., Lynch W.* Determination of Equation of State of Dense Matter // *Science*. 2002. V. 298. P. 1592.
2. *Zhang Y., Li Z.* Elliptic Flow and System Size Dependence of Transition Energies at Intermediate Energies // *Phys. Rev. C*. 2006. V. 74. P. 014602;
Zhang M. W. et al. Onset of Flow of Charged Fragments in Au–Au Collisions // *Phys. Rev. C*. 1990. V. 42. P. R491;
Beavis D. et al. Collective Motion in Ar + Pb Collision at Beam Energies between 400 and 1800 MeV/nucleon // *Phys. Rev. C*. 1999. V. 45. P. 299.
3. *Hong B. et al.* Charged Pion Production in $^{96}\text{Ru} + ^{96}\text{Ru}$ Collisions at 400A and 1528A MeV // *Phys. Rev. C*. 2005. V. 71. P. 034902.
4. *Pan Q., Danielewicz P.* From Sideward Flow to Nuclear Compressibility // *Phys. Rev. Lett.* 1993. V. 70. P. 2062;
Ramillien V. et al. Sideward Flow in Au + Au Collisions at 400A MeV // *Nucl. Phys. A*. 1995. V. 587. P. 802.
5. *Lukasik J. et al.* Directed and Elliptic Flow in $^{197}\text{Au} + ^{197}\text{Au}$ at Intermediate Energies // *Phys. Lett. B*. 2005. V. 608. P. 223.
6. *Ogilvie C. A. et al.* Transverse Collective Motion in Intermediate-Energy Heavy-Ion Collisions // *Phys. Rev. C*. 1989. V. 40. P. 2592;
Blättel B. et al. Origin of Transverse Momentum in Relativistic Heavy-Ion Collisions: Microscopic Study // *Phys. Rev. C*. 1991. V. 43. P. 2728.
7. *Andronic A. et al.* Directed Flow in Au + Au, Xe + CsI and Ni + Ni Collisions and the Nuclear Equation of State // *Phys. Rev. C*. 2003. V. 67. P. 034907;
Sood A. D., Puri R. K. Mass Dependence of Disappearance of Transverse In-plane Flow // *Phys. Rev. C*. 2004. V. 69. P. 054612; Systematic Study of the Energy of Vanishing Flow: Role of Equations of State and Cross-Sections // *Phys. Rev. C*. 2006. V. 73. P. 067602; Influence of Momentum-Dependence Interactions on Balance Energy and Mass Dependence // *Eur. Phys. J. A*. 2006. V. 30. P. 571.
8. *Goyal S.* Role of Colliding Geometry on the Balance Energy of Mass-Asymmetric Systems // *Phys. Rev. C*. 2011. V. 83. P. 047604;
Goyal S., Puri R. K. On the Sensitivity of the Energy of Vanishing Flow towards Mass Asymmetry of Colliding Nuclei // *Nucl. Phys. A*. 2011. V. 853. P. 164.
9. *Li B. A. et al.* Isospin Dependence of Collective Flow in Heavy-Ion Collisions at Intermediate Energies // *Phys. Rev. Lett.* 1996. V. 76. P. 4492.
10. *Pak R. et al.* Isospin Dependence of Collective Transverse Flow in Nuclear Collisions // *Phys. Rev. Lett.* 1997. V. 78. P. 1022; Isospin Dependence of the Balance Energy // *Ibid.* P. 1026.

11. *Gautam S. et al.* Sensitivity of the Transverse Flow to the Symmetry Energy // *Phys. Rev. C.* 2011. V. 83. P.034606;
Kaur V., Kumar S., Puri R. K. On the Elliptical Flow and Asymmetry of the Colliding Nuclei // *Phys. Lett. B.* 2011. V. 697. P.512.
12. *Krofcheck D. et al.* Disappearance of Flow in Heavy-Ion Collisions // *Phys. Rev. Lett.* 1989. V. 63. P.2028.
13. *Westfall G. D. et al.* Mass Dependence of Disappearance of Flow in Nuclear Collisions // *Phys. Rev. Lett.* 1993. V. 71. P.1986;
Buta A. et al. Azimuthal Correlation Functions and the Energy of Vanishing Flow in Nucleus–Nucleus Collisions // *Nucl. Phys. A.* 1995. V. 584. P.397.
14. *Sood A. D., Puri R. K.* Systematic Study of Energy of Vanishing Flow: Role of Equations of State and Cross-Sections // *Phys. Rev. C.* 2006. V. 73. P.067602;
Majestro D. J. et al. Disappearance of Flow in Au + Au Collisions // *Phys. Rev. C.* 2000. V. 61. P.021602(R);
Sood A. D., Puri R. K. Nuclear Dynamics at the Balance Energy // *Phys. Rev. C.* 2004. V. 70. P.034611;
Kumar S. et al. Impact Parameter Dependence of the Disappearance of Flow and In-medium Nucleon–Nucleon Cross-Section // *Phys. Rev. C.* 1998. V. 58. P.3494.
15. *Scalone L., Colonna M., Di Toro M.* Transverse Flows in Charge Asymmetric Collisions // *Phys. Lett. B.* 1991. V. 461. P.9.
16. *Gautam S. et al.* Isospin Effects on the Energy of Vanishing Flow in Heavy-Ion Collisions // *J. Phys. G: Nucl. Part. Phys.* 2010. V. 37. P.085102;
Gautam S., Sood A. D. Isospin Effects on the Mass Dependence of the Balance Energy // *Phys. Rev. C.* 2010. V. 82. P.014604;
Gautam S. et al. Isospin Effects in the Disappearance of Flow as a Function of Colliding Geometry // *Phys. Rev. C.* 2011. V. 83. P.014603;
Gautam S., Puri R. K. Participation-Spectator Matter and Thermalization of Neutron-Rich Systems at the Energy of Vanishing Flow // *Phys. Rev. C.* 2012. V. 85. P.067601;
Gautam S., Kumari R., Puri R. K. Sensitivity of Transverse Flow toward Isospin-Dependent Cross-Sections and Symmetry Energy // *Ibid.* V. 86. P. 034607.
17. *Kumar S. et al.* Elliptic Flow and Isospin Effects in Heavy-Ion Collisions at Intermediate Energies // *Phys. Rev. C.* 2010. V. 81. P.014611.
18. *Kumar S., Puri R. K.* Effect of Symmetry Energy on Nuclear Stopping and Its Relation to the Production of Light Charged Fragments // *Ibid.* P.014601.
19. *Chugh R., Sood A. D.* Geometry of Vanishing Flow: A New Probe to Determine the In-medium Nucleon–Nucleon Cross-Section // *Parma. J. Phys.* 2011. V. 77. P.289;
Goyal S. Role of the Mass Asymmetry of Reaction on the Geometry of Vanishing Flow // *Nucl. Phys. A.* 2011. V. 856. P.154.
20. *Aichelin J., Stöcker H.* Quantum Molecular Dynamics — A Novel Approach to N -Body Correlations in Heavy-Ion Collisions // *Phys. Lett. B.* 1986. V. 176. P.14.
21. *Cugnon J., Mizutani T., Vandermeulen J.* Equilibrations in Relativistic Nuclear Collisions. A Monte Carlo Calculation // *Nucl. Phys. A.* 1981. V. 352. P.505.
22. *Lehmann E. et al.* Consequences of a Covariant Description of Heavy-Ion Reactions at Intermediate Energies // *Phys. Rev. C.* 1995. V.51. P.2113; Relativistic versus Nonrelativistic Quantum Molecular Dynamics // *Prog. Part. Nucl. Phys.* 1993. V. 30. P.219.

Received on April 10, 2013.